

## **FFI RAPPORT**

### **MATERIAL PROPERTIES OF WOLFRAM CARBIDE ESTABLISHED BY USING A BENDING TEST**

NILSSEN Jan R, MOXNES John F, SAGSVEEN Bendik A

**FFI/RAPPORT-2002/02387**



FFIBM/778/130

Approved  
Kjeller 3 May 2002

Bjarne Haugstad  
Director of Research

**MATERIAL PROPERTIES OF WOLFRAM  
CARBIDE ESTABLISHED BY USING A BENDING  
TEST**

NILSSEN Jan R, MOXNES John F,  
SAGSVEEN Bendik A

FFI/RAPPORT-2002/02387

**FORSVARETS FORSKNINGSINSTITUTT**  
**Norwegian Defence Research Establishment**  
P O Box 25, NO-2027 Kjeller, Norway



**FORSVARETS FORSKNINGSINSTITUTT (FFI)**  
**Norwegian Defence Research Establishment**

**UNCLASSIFIED**

P O BOX 25  
 NO-2027 KJELLER, NORWAY  
**REPORT DOCUMENTATION PAGE**

**SECURITY CLASSIFICATION OF THIS PAGE**  
 (when data entered)

1) PUBL/REPORT NUMBER FFI/RAPPORT-2002/02387 1a) PROJECT REFERENCE FFIBM/778/130	2) SECURITY CLASSIFICATION UNCLASSIFIED 2a) DECLASSIFICATION/DOWNGRADING SCHEDULE -	3) NUMBER OF 15
4) TITLE MATERIAL PROPERTIES OF WOLFRAM CARBIDE ESTABLISHED BY USING A BENDING TEST		
5) NAMES OF AUTHOR(S) IN FULL (surname first) NILSSEN Jan R ,MOXNES John F, SAGSVEEN Bendik A		
6) DISTRIBUTION STATEMENT Approved for public release. Distribution unlimited. (Offentlig tilgjengelig)		
7) INDEXING TERMS IN ENGLISH:		
IN NORWEGIAN:		
a) <u>Wolfram Carbide</u> b) <u>Bending test</u> c) <u>Inverse modeling</u> d) _____ e) _____	a) <u>Wolfram karbid</u> b) <u>Bøyetest</u> c) <u>Invers modellering</u> d) _____ e) _____	
THESAURUS REFERENCE:		
8) ABSTRACT  In this article a study of the stresses caused by bending of penetrators made of Wolfram Carbide has been carried out. Experimental data was compared with simulations using the Marc-3D code and with solutions from a simple analytical bending theory. The Marc-3D simulations gave good agreement with the experimental results and with results from the analytical theory. By using an inverse modelling technique the fracture stress of the Wolfram Carbide was established.		
9) DATE  3 May 2002	AUTHORIZED BY This page only  Bjarne Haugstad	POSITION  Director of Research

**UNCLASSIFIED**

**SECURITY CLASSIFICATION OF THIS PAGE**  
 (when data entered)



## CONTENTS

	<b>Page</b>
1 INTRODUCTION	7
2 THE SET-UP	8
3 THE LINEAR ANALYTICAL BENDING THEORY	8
4 MARC RESULTS, ANALYTICAL RESULTS AND EXPERIMENTAL RESULTS	9
5 CONCLUSION/DISCUSSION	12
References	13
A APPENDIX	14
Distribution list	15





## **MATERIAL PROPERTIES OF WOLFRAM CARBIDE ESTABLISHED BY USING A BENDING TEST**

### **1 INTRODUCTION**

The Norwegian armed forces use the Multipurpose (MP) 12.7 ammunition. Nammo Raufoss AS is the inventor of the MP concept, and the MP technology was developed during the end of the 60s. The first series production started in the beginning of the 70s.

In earlier studies [1], the penetration capabilities of the hard core of the 12.7 MP round, made of Wolfram Carbide, has been carried out. It was found that the hardness of the Wolfram Carbide was larger than predicted by tensile tests. This is not surprising since a difference between the fracture stress in tension and compression (created during penetration) is to be expected for brittle materials. For glass the difference is approximately a factor of ten.

In order to analyze the fracture stress of Wolfram Carbide during compression, an ordinary indentation test of the Wolfram carbide penetrating into a steel target was carried out in [2]. Simulation results from the Nike-2D [3] were compared with experimental results from the test, and with numerical results from a standard theory of indentation. The Nike-2D simulations showed good agreement with experiments.

New experiments at NDRE reveal [4] that during indentation, the penetrator first penetrates the steel block without being plastically deformed. Thereafter, fracturing appears at an axial force of 156 kN. The piecewise conical nose of the penetrator is then 5.3 mm into the steel block, and the radius of the projected contact area along the direction of indentation is 3 mm, which corresponds to a fracture stress of 5.5 GPa and a pressure of 1.8 GPa. The nose is completely surrounded when the projected radius is 3.5 mm. Complete indentation of the penetrator nose into the target is probably not possible without causing fracturing of the penetrator. Also, the dynamic forces are small compared to the static strength forces during dynamic penetration into steel targets by projectiles with initial velocities about 900m/s. Most likely, the projectile should therefore also fracture during dynamic penetration. This conclusion is supported by experiments showing that projectiles, which impact the target with non-zero Yaw angles, have strongly reduced penetration depths [1].

In order to analyze the penetration capabilities by using computer codes, the material model of Wolfram Carbide is important to construct. We hypothesize that the fracture stress is dependent of the pressure, where increased pressure leads to increased fracture stress. The bending test used in this article pinpoints one point on the fracture/pressure curve by assuming that the fracture stress is related to a critical Mises stress.

## 2 THE SET-UP

In Figure 2.1 the numerical set-up of the experimental situation is shown.

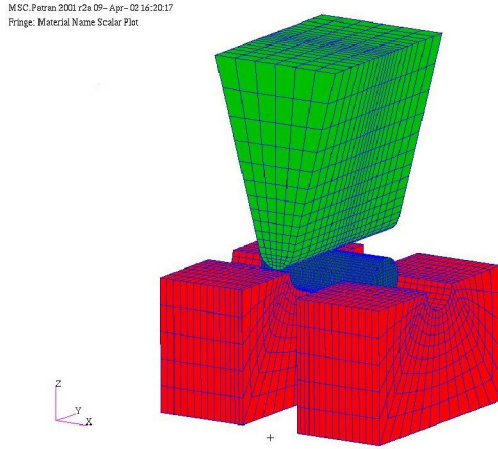


*Figure 2.1 The set-up of the bending test of the projectile hard core. The experimental recording was the force on the top of the piston and the displacement of the top of the piston.*

A piston made of steel bends the penetrator. The numerical results are found by using the Marc-3D hydro code [5]. Both the piston and the supporting steel blocks are modeled as elastic-plastic steel materials. The penetrator is modeled as an elastic material up to the fracture stress.

The numerical model is built up from 8-noded brick-elements, with a total of 22280 elements and 26171 nodes. The supporting steel blocks are fully constrained at their bottom surfaces. The Wolfram Carbide penetrator is lying free in its supports, with a 10mm gap between the two blocks. The piston is moving vertical downwards with a speed of 1mm/sek, applying a symmetric load to the penetrator. All contact bodies in the numerical analysis are modelled as "deformable bodies". An "Iterative Sparse" type solver with "Incomplete Cholesky" preconditioner is used.

## 3 THE LINEAR ANALYTICAL BENDING THEORY

This section gives a short analytical presentation of the bending test.

Assume that a rod of circular cross section with length  $l$  (the distance between the supporting steel blocks) is bent by a force  $f$  applied to its mid-point. During bending the rod is stretched at some points and compressed at others. The neutral surface of the rod separates the region of compression from the region of extension.

The solution of the bending displacement of the neutral surface is given by  $\zeta(x)$ , where  $x$  is the distance along the rod. The familiar linear bending equation is

$$\zeta(x)^{(4)} = 0, \text{ when } x \neq l/2 \quad (3.1)$$

At  $x = l/2$ ,  $\zeta, \zeta'$  and  $\zeta^{(2)}$  are continuous, while the discontinuity of the shearing force,  $-EI\zeta^{(3)}$ , is equal to the applied force  $f$ .  $E$  is Young's modulus of the rod, and  $I$  is the principal moments of inertia about any axis lying in the circular cross section. A circular rod has  $I = (1/4)\pi a^4$ , where  $a$  is the radius of the rod. By assuming supporting edges, i.e.  $\zeta(0) = \zeta(l) = 0$ , the general solution of the displacement is

$$\zeta(x) = f(4l^2x - 4x^3)/(48EI), \zeta(l/2) = fl^3/(48EI), \quad I = (1/4)\pi a^4 \quad (3.2)$$

Observe the linearity between the force and the displacement.

The bending stress is given as

$$\sigma(x, z) = E z / R(x) \approx E\zeta''(x) z \quad (3.3)$$

where  $z$  is the distance from the neutral surface in the rod, and  $R$  is the radius of curvature of the neutral surface of the rod. Using relation (3.2) in (3.3) and letting  $z = a$  gives the maximal bending stress (tension) when  $x = l/2$  as

$$\sigma = E\zeta''a = (1/4)fla/I \Rightarrow f = 4\sigma I/(la) \quad (3.4)$$

Observe again the linearity between the stress and the force. Observe that the displacement is absent in this formulae.

#### 4 MARC RESULTS, ANALYTICAL RESULTS AND EXPERIMENTAL RESULTS

In this section simulations with Marc-3D are compared with experiments and with results from the analytical theory (equation (3.4)). The material parameters are given in appendix A. Figure 4.1 shows the force on the piston as a function of the displacement of the piston. Unknown numerical effects probably cause the scattering in the numerical curve, but in general, good match between the experiments and the numerical solution is achieved. The results show that the computer model is viable and can be used in further stress studies. The hardcore fractured for two identical tests when the force was 40.08kN and 38.29kN.

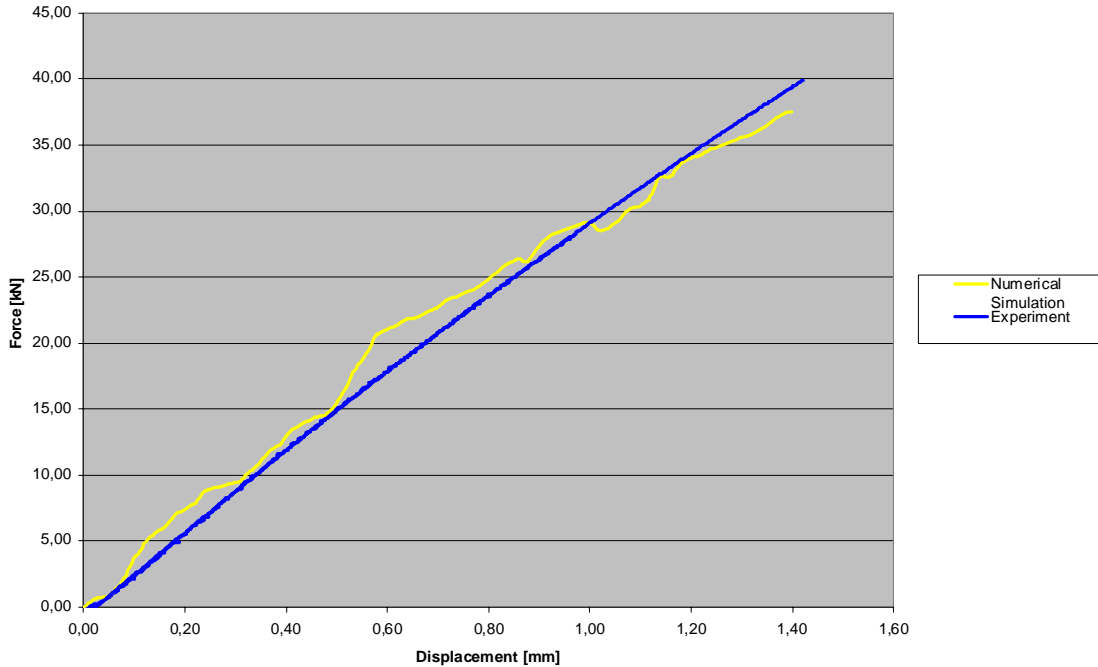


Figure 4.1 The experimental and numerical force as a function of the displacement of the piston.

Figure 4.2 shows the force as a function of the simulated Mises stress in the critical element of the rod. Observe the close agreement between the analytical solution in (3.4) and the numerical solution. The bending of the hardcore is small and close agreement with the numerical results is accordingly expected. By comparing Figure 4.1 and Figure 4.2, observe that the Mises stress was close to 2.75GPa when the hardcore fractured. Figure 4.3 shows a picture of the penetrator after fracturing. The fractured zone is just below the mid-point of the penetrator where the force was acting. As expected, the fracture zone is in the vertical direction of the rod. The principal bending stress along the direction of the rod is much larger than the other stresses, giving essentially a simple tension situation in the critical element of the rod. The rod will most easily fracture in the state of maximal tension.

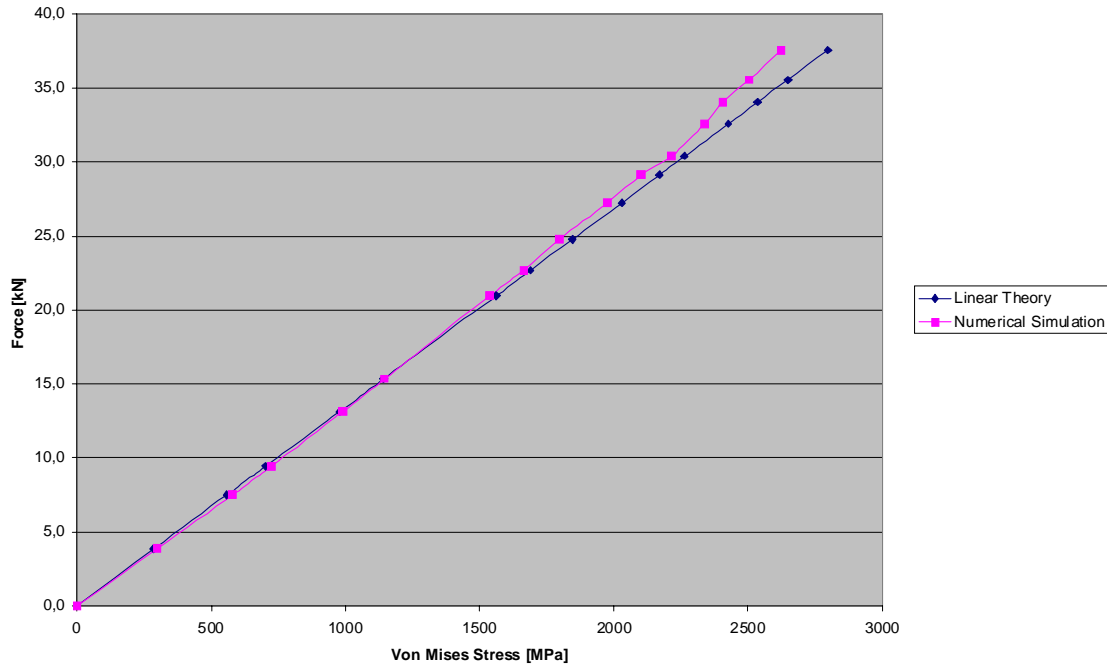


Figure 4.2 The simulated and analytical force on the piston as a function of the Mises stress in the critical region of the penetrator.



Figure 4.3 The penetrator after being fractured.

Figure 4.4 shows the Mises as a function of the pressure. By comparing Figure 4.2 with Figure 4.4, observe that that the pressure was 0.9 GPa when the rod fractured. Also observe that the pressure is approximately minus one third of the Mises stress, showing the almost pure simple tension situation.

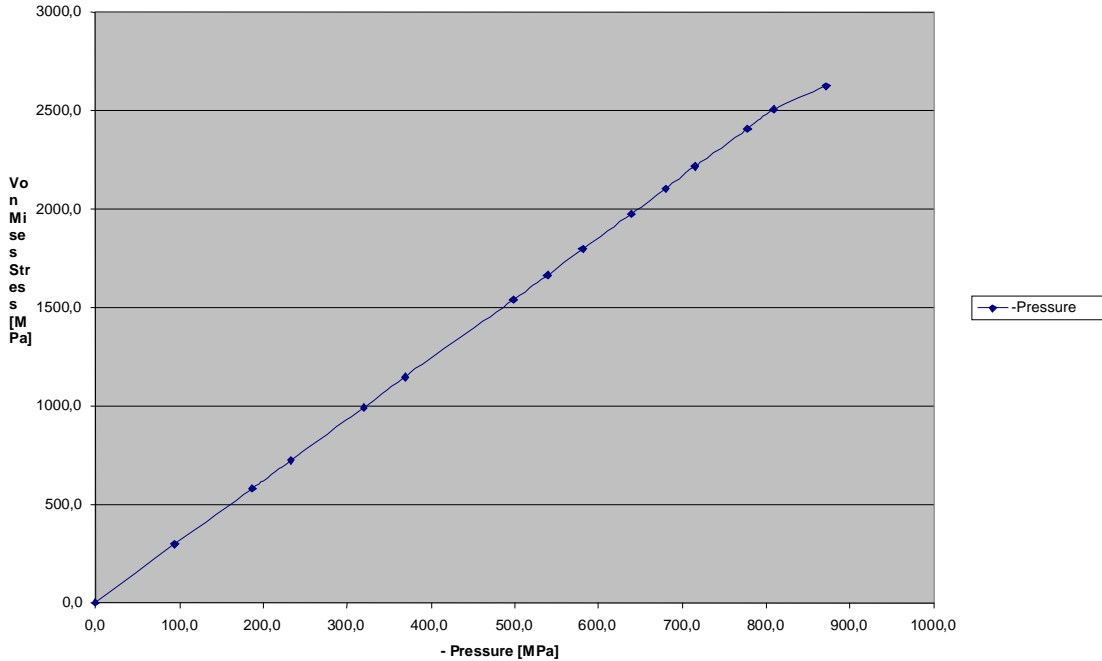


Figure 4.4 The Mises stress in the critical region as a function of -pressure.

Summing up: We have found a point on the fracture curve (the critical Mises stress as a function of pressure) given as ( -0.9 GPa, 2.75 GPa). The numerical solution is in agreement with the analytical solution.

## 5 CONCLUSION/DISCUSSION

We found in the last section that the Marc-3D results and the results from the analytical theory showed good agreement with experiments. The bending test, which corresponds to a simple tension situation, gives the point ( -0.9 GPa, 2.75 GPa) in the Mises/pressure fracture diagram. Also a simple compression test gives the point (1.8 GPa, 5.5 GPa) in the same diagram. Drawing a straight line between those two points gives a curve that crosses the horizontal axis at a pressure of approximately -3 GPa, corresponding to the fracture pressure during pure tension. The literature shows fractures stress in the range of 2.7 GPa –6.6 GPa during simple compression, while one values is reported as 0.3 GPa during simple tension. Sandvik Hard Materials, Norway, report 2.4 GPa for the critical Mises stress during bending. This value is somewhat lower than our value of 2.75GPa. Nammo Raufoss reports a point (0.53 GPa, 1.6 GPa) during simple tension of the hardcore, which is approximately a factor of two lower than our result during simple tension during bending. Further studies are necessary to clear up the discrepancy.

## References

- [1] Diep Q.B., Moxnes J. F., Penetration of multipurpose projectiles into steel targets, Nammo Raufoss document, 6585070-961,2001.
- [2] Diep Q.B., Nilsen J.R., Moxnes J. F., Inverse modeling of indentation into steel plates, Nammo Raufoss document, 6585070-912,2001.
- [3] HI NIKE2D: PC version developed by Ph.D. Michael I. Murphy of Hydrosoft International of the public domain NIKE2D code developed at the Lawrence Livermore National Laboratory.
- [4] Nilssen J.R., Moxnes J. F., Fracture stress of Wolfram Carbide during simple compression, Forthcoming.
- [5] MSC.Marc Theory & User Information, Version 2001, Msc.Software.

**Acknowledgement:** We thank Tor Alexander Fjeldly at FFI for helping us with the input to the Marc 3D code.

## A APPENDIX

Penetrator: (H10N)

Density:  $14.55\text{g/cm}^3$  (measured at FFI), 89-91% WC, 9-11% Co, C max 0.03%, Fe max 0.35%, Titan and Tantalum max 0.5%, Hardness 89+-2 HRA,

Particle diameter: Less than 8 micron,

Youngs modulus:  $E= 367\text{ GPa}$ , Poison relation: 0.20

Radius: 3.5 mm, Bending length: 1.0 cm

Sandvik Hard Materials report (H10N): Density:  $14.25\text{g/cm}^3$ , Youngs modulus:  $E= 585\text{ GPa}$ , Poison relation: 0.22

Supporting blocks:

Density:  $7.9\text{g/cm}^3$ , Youngs modulus:  $E= 210\text{ GPa}$ , Poison relation: 0.30

Yield function ( Elastic-Plastic, piece wise linear): Plastic Strain: 0.0, 0.05, 0.11, 0.2, 0.4, 0.6, 0.8, 1.0, 2.0, 3.5. Stress (GPa): 1.1,1.19, 1.224, 1.25, 1.3, 1.333, 1.371, 1.404, 1.584, 1.814.

Piston:

Density:  $7.9\text{g/cm}^3$ , Youngs modulus:  $E= 206\text{ GPa}$ , Poison relation: 0.30

Yield function ( Elastic-Plastic, piece wise linear): Plastic Strain: 0.0, 0.05, 0.11, 0.2, 0.4, 0.6, 0.8, 1.0, 2.0, 3.5. Stress (GPa): 0.674, 0.684, 0.699, 0.731, 0.759, 0.785, 0.813, 0.939, 1.115.



## DISTRIBUTION LIST

**FFIBM**      **Dato:** 3 mai 2002

RAPPORTTYPE (KRYSS AV)		RAPPORT NR.	REFERANSE	RAPPORTENS DATO	
<input checked="" type="checkbox"/> RAPP	<input type="checkbox"/> NOTAT	<input type="checkbox"/> RR	2002/02387	FFIBM/778/130	3 mai 2002
RAPPORTENS BESKYTTELSESGRAD			ANTALL EKS UTSTEDT	ANTALL SIDER	
Unclassified			39	15	
RAPPORTENS TITTEL			FORFATTER(E)		
MATERIAL PROPERTIES OF WOLFRAM CARBIDE ESTABLISHED BY USING A BENDING TEST			NILSSEN Jan R. MOXNES John F, SAGSVEEN Bendik		
FORDELING GODKJENT AV FORSKNINGSSJEF			FORDELING GODKJENT AV AVDELINGSSJEF:		
Bjarne Haugstad			Jan Ivar Botnan		

### EKSTERN FORDELING

### INTERN FORDELING

ANTALL	EKS NR	TIL	ANTALL	EKS NR	TIL
1		Nammo Raufoss AS	14		FFI-Bibl
1		Monika Stømgård	1		Adm direktør/stabssjef
1		Gard Ødegårdstuen	1		FFIE
1		Eva Friis	1		FFISYS
1		Quac Bao Diep	1		FFIN
		Postboks 162	1		Bjarne Haugstad, FFIBM
		2831 Raufoss	1		Svein W Eriksen, FFIBM
			1		John F. Moxnes, FFIBM
1		Naval Air Warfare Center Weapons Division, China Lake, CA 93555-6100 US	1		Gunnar Ove Nevstad, FFIBM
			6		FFIBM
1		Alice I. Atwood			FFI-veven
1		Allen Lindfors			
1		Combustion Research Section Naval Air Warfare Center Weapons Division, Code 4T4310D, 1 Administration Circle China Lake, CA 93555-6100 US			
1		NAWC, Crane			
1		David Holt			

FFI-K1      Retningslinjer for fordeling og forsendelse er gitt i Oraklet, Bind I, Bestemmelser om publikasjoner for Forsvarets forskningsinstitutt, pkt 2 og 5. Benytt ny side om nødvendig.